NASA TECHNICAL MEMORANDUM

NASA TM X-2818

NASA TM X-2818

TERMINAL SHOCK POSITION AND RESTART CONTROL OF A MACH 2.7, TWO-DIMENSIONAL, TWIN-DUCT MIXED-COMPRESSION INLET

by Gary L. Cole, George H. Neiner, and Robert J. Baumbick

Lewis Research Center
Cleveland, Ohio 44135

NATIONAL AERONAUTICS AND SPACE ADMINISTRATION • WASHINGTON, D. C. • JUNE 1973

1. Report No.	2. Government Accession No.	3. Recipient's Catalog No.
NASA TM X-2818		

4. Title and Subtitle	5. Report Date
TERMINAL SHOCK POSITION AND RESTART CONTROL OF A MACH 2.7, TWO-DIMENSIONAL, TWIN-DUCT MIXED-COMPRESSION INLET	June 1973
	6. Performing Organization Code
7. Author(s)	8. Performing Organization Report No.
Gary L. Cole, George H. Neiner, and Robert J. Baumbick	E-7223
	10. Work Unit No.
9. Performing Organization Name and Address	501-24
Lewis Research Center National Aeronautics and Space Administration Cleveland, Ohio 44135	11. Contract or Grant No.
	13. Type of Report and Period Covered
12. Sponsoring Agency Name and Address	Technical Memorandum
National Aeronautics and Space Administration Washington, D.C. 20546	14. Sponsoring Agency Code

15. Supplementary Notes

16. Abstract

Experimental results of terminal shock and restart control system tests of the inlet are presented. High-response (110-Hz bandwidth) overboard bypass doors were used, both as the variable to control shock position and as the means of disturbing the inlet airflow. An inherent instability in inlet shock position resulted in noisy feedback signals and thus restricted the terminal shock position control performance that was achieved. Proportional-plus-integral-type controllers using either throat exit static pressure or shock position sensor feedback gave adequate low-frequency control. The inlet restart control system kept the terminal shock control loop closed throughout the unstart-restart transient. The capability to restart the inlet was not limited by the inlet instability.

17. Key Words (Suggested by Author(s))	18. Distribution Statement
Automatic control; Supersonic inlets; Air intake system; Supersonic inlet control; Normal shock control; Terminal shock control; Restart control	Unclassified - unlimited

19. Security Classif. (of this report)	20. Security Classif. (of this page)	21. No. of Pages	22. Price*
Unclassified	Unclassified	44	$3.00

* For sale by the National Technical Information Service, Springfield, Virginia 22151

CONTENTS

TERMINAL SHOCK POSITION AND RESTART CONTROL OF A MACH 2.7, TWO-DIMENSIONAL, TWIN-DUCT MIXED-COMPRESSION INLET

by Gary L. Cole, George H. Neiner, and Robert J. Baumbick

Lewis Research Center

SUMMARY

Experimental frequency response test results of an inlet terminal shock control system and transient tests of an inlet restart control system are presented. High-response (110-Hz bandwidth) overboard bypass doors were used as the variable to control shock position and as the means of disturbing inlet airflow. An inherent instability in inlet shock position resulted in noisy feedback signals, which restricted the terminal shock position control performance that was achieved. But the restart capability of the control system did not seem to be affected by the noisy signals.

Proportional-plus-integral-type terminal shock control gave somewhat better performance with throat exit static pressure feedback than with shock position sensor feedback. Closed-loop attenuation of disturbance-induced shock motion below open-loop values was achieved from 0 to 15 hertz with pressure feedback and from 0 to 8.5 hertz with shock sensor feedback.

A proportional loop feeding back a diffuser exit pressure was added in an attempt to improve control performance by feeding back a signal closer to the disturbance. Closed-loop frequency response data did indicate an improvement. The addition of the proportional loop resulted in much more noise being propagated through the control system and an accompanying increase in undesired bypass door activity. Since the increase in bypass door activity was considered unacceptable, the proportional loop was eliminated.

The inlet restart control system kept the terminal shock control loop closed throughout the unstart-restart transient. This was accomplished by scheduling the shock controller setpoint. A proportional-plus-integral controller (using pressure feedback) was used for each duct, since either or both ducts could be unstarted. Tests were conducted with the inlet ramp at two different initial positions. In one case it was necessary to collapse the ramp to effect a restart. The unstart-restart cycle time was much shorter and the control system was simpler when the ramp did not have to be collapsed (larger initial throat area). These advantages may be offset by a loss in compressor face total pressure recovery of about 4 percent caused by the increase in throat Mach number.

INTRODUCTION

The basic function of an inlet is to change the kinetic energy of the free-stream air to potential energy, thus increasing the static pressure of the air. Ideally, the inlet will do this with a minimum loss in total pressure recovery and will provide a uniform (low distortion) total pressure distribution at the compressor face station. Generally speaking, for inlets with internal supersonic compression, total pressure recovery increases and distortion decreases as the terminal shock is moved closer to the inlet's throat. Thus, a shock operating point close to the throat is desirable. However, airflow disturbances can displace the shock from its operating point. An upstream displacement could result in an inlet unstart. An unstart transient can have drastic effects on the propulsion system such as compressor stall and combustor flameout, and on the aircraft itself because of the sudden increase in drag of the unstarted inlet. A downstream shock displacement would result in a decrease of propulsion system performance because of the lower pressure recovery and higher distortion. A large downstream displacement could conceivably result in a distortion-induced compressor stall followed by an inlet unstart. The tolerance of the inlet against unstarts caused by a sudden mismatch between inlet and engine airflows can be increased by moving the terminal shock operating point further downstream of the throat. But this also decreases propulsion system performance. By providing the inlet with a terminal shock control system, the terminal shock distance from the throat can be reduced while an increased tolerance against unstart is maintained.

Some previous efforts to increase inlet stability and control shock position are listed here for reference. Passive-type control devices, such as throat bleed systems and vortex valves, for increasing inlet stability were investigated and are reported in reference 1. A control system using overboard bypass doors to control the terminal shock and a study of feedback control signals are reported in reference 2. Both analog and digital control of an axisymmetric mixed-compression inlet have been investigated at the Lewis Research Center (refs. 3 and 4). These investigations utilized high-response (110-Hz bandwidth) overboard bypass doors as the manipulated variable of the terminal shock controller. The inlet itself had a bandwidth of approximately 55 hertz.

An inlet control system should include the capability to restart the inlet (in the event that an unstart occurs), as well as provide terminal shock position control.

In addition, it is desirable to keep the terminal shock control loop closed throughout an unstart-restart transient. Thus, it is possible to maintain a match between inlet airflow and engine airflow and, hence, maintain reasonably high total pressure recovery and low distortion at the engine compressor face. Such a control system for a mixed-compression axisymmetric inlet is reported in reference 5.

The controls investigation reported herein represents only part of a dynamics, controls, and terminal shock position sensing program for the Mach 2.7, two-dimensional inlet. The results of a program to obtain open-loop responses of various inlet static pressures and the terminal shock position to overboard bypass door disturbances are reported in reference 6. An investigation of electronic shock position sensors using cowl static pressures is reported in reference 7. Steady-state performance of the inlet was investigated during another program. The results have not been published to date.

In general, the objectives of the control program were to investigate ways of improving terminal shock and restart control systems for inlets with internal supersonic compression. One possibility prior to the test program was to improve the two-loop terminal shock control reported in reference 3. Analytical studies indicated that this might be possible. Another possibility was to investigate the use of a terminal shock position sensor having an electronic output as a feedback signal in the shock control system. Thirdly, it was desired to minimize the setpoint scheduling of the shock controller that was used with the restart control system.

There were also some test objectives that were specifically related to the inlet configuration. The inlet is a two-dimensional type with two ducts separated by a ramp centerbody and a splitter plate extending from the aft end of the centerbody. Each duct had its own terminal shock to be controlled. Because of a back-pressured throat bleed system, airflow coupling between the two ducts and thus interaction of the two shocks was possible. Therefore, another objective was to investigate having to control two shocks instead of one, as in an axisymmetric inlet. Also, the restart control problem for this inlet is more complicated because either or both ducts could be in an unstarted condition. Thus, it was desired to investigate unstart transients in either or both ducts. There was also interest in investigating operation of the inlet in a self-starting configuration (no need to collapse ramp to effect restart) because of the faster restart transient and simpler control requirements.

The subject matter contained within this report and the organization of the material is as follows:

(1) A description of the inlet that was tested and the control hardware that was used

(2) A description of test procedures that were used

(3) A presentation of inlet open-loop characteristics, including steady-state gains and dynamics of shock position and two static pressures (potential control signals) to overboard bypass door disturbances; and a description of an inherent inlet shock instability

(4) Experimental closed-loop frequency response results and discussion of the terminal shock control systems that were tested, with an emphasis on problems due to signal noise resulting from the shock instability

(5) A discussion of the restart control system and experimental unstart-restart transient results

APPARATUS

Inlet

Figure 1 shows the inlet used during the investigation mounted in the 10- by

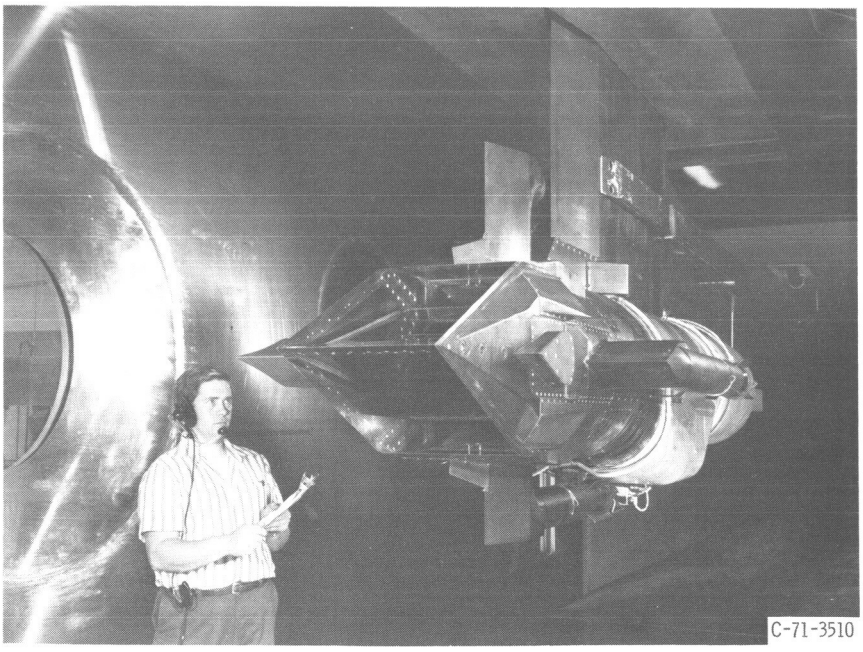

Figure 1. - Installation of Mach 2.7 two-dimensional mixed-compression inlet in 10- by 10-foot Supersonic Wind Tunnel.

10-Foot Supersonic Wind Tunnel at the Lewis Research Center. The inlet is a two-dimensional type with twin ducts and a collapsible ramp centerbody. Seventy percent of the supersonic area contraction occurs externally at the inlet design Mach number of 2.7.

The inlet has a capture area of 2210 square centimeters and is sized for operation with a J85-13 turbojet engine. The inlet was terminated by a choked orifice plate during this investigation. The plate had a flow area of approximately 590 square centimeters (equivalent to a corrected airflow of 14.2 kg/sec). It was located 136 centimeters downstream of the cowl lip, approximately the same location as the J85 compressor face station. This configuration was chosen because, as was shown in reference 8, the dynamics of an inlet terminated by a choked orifice plate at the compressor face station are very similar to the dynamics of the inlet coupled to a J85-13 turbojet engine. The overall length of the inlet is roughly one-half that of a single-duct inlet which would supply the same total airflow. Thus the inlet is suitable for an under-the-wing installation which shields the inlet during angle-of-attack maneuvers. The inlet would then be mounted with the ramp in a vertical position so that maximum tolerance to sideslip can be achieved by varying ramp position. As can be seen from figure 1 the inlet was mounted in the tunnel with the ramp in a horizontal position. Therefore inlet tolerance to sideslip could be investigated by varying the pitch angle of the inlet.

Inlet Systems

Performance bleed. - The inlet had a performance bleed system (fig. 2), for boundary-layer control and to increase stability, which consisted of rows of holes 0.317 centimeter in diameter on the ramp, cowl, and sidewall surfaces. The forward ramp bleed was ducted overboard through pipes, as shown in figure 2. The throat bleed (all surfaces) was ducted to a common plenum and then dumped overboard through four pipes (two of which can be seen in fig. 2). The exit area of the pipes could be varied by means of remotely controlled plugs, thus allowing the throat bleed system to be backpressured. This can result in unchoking of the bleed holes and possibly permit airflow coupling between the terminal shocks of the two ducts. The throat bleed was backpressured during all tests conducted during this program.

Vortex generators. - Vortex generators were located on the inlet's cowl, sidewall, and ramp surfaces, as shown in figure 2. The primary purpose of the vortex

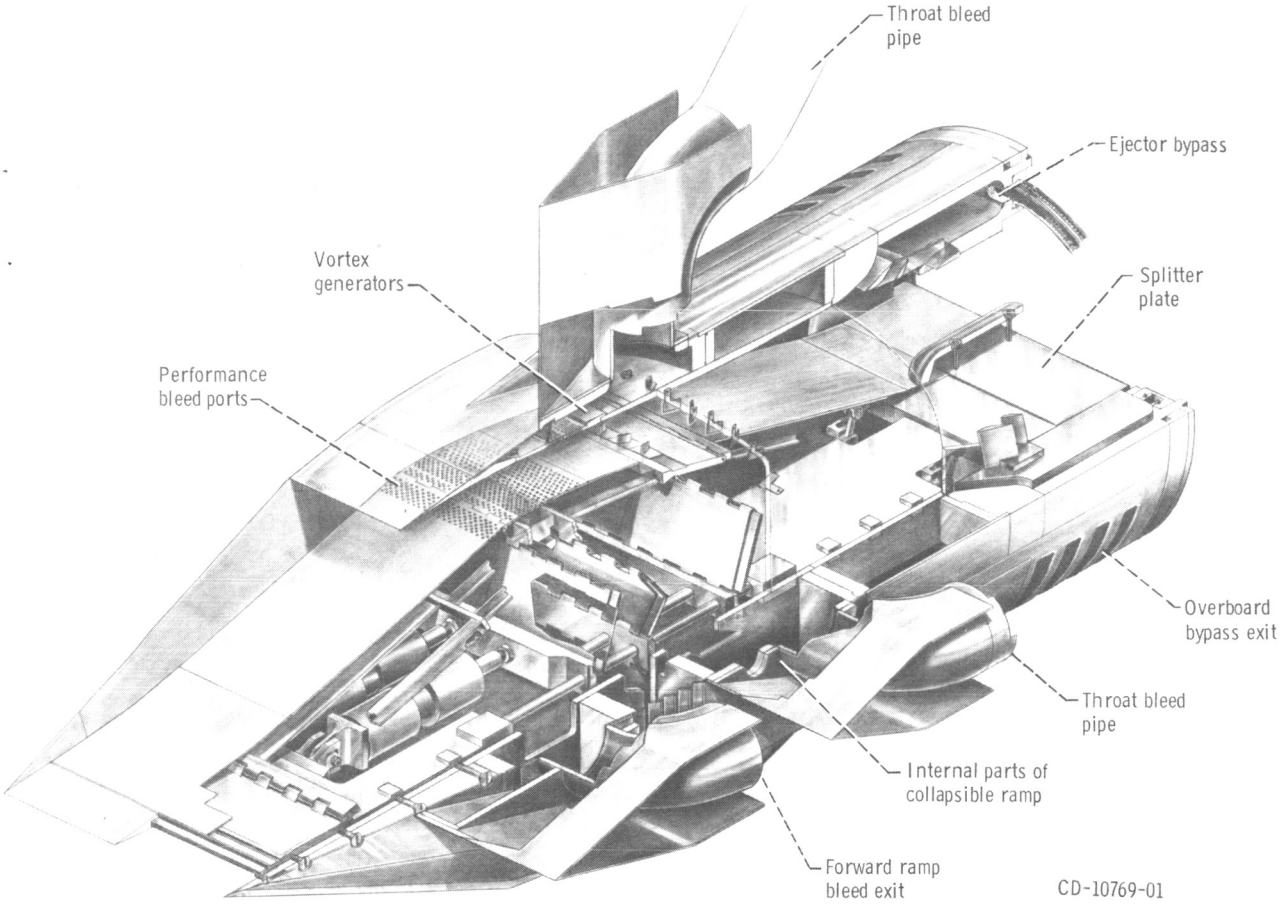

Figure 2. - Cutaway view of the two-dimensional inlet.

generators was to delay boundary-layer separation in the subsonic diffuser. This helped to achieve a more uniform total pressure distribution (less distortion) at the compressor face.

Collapsible ramp. - The ramp could be expanded or collapsed by means of an electrohydraulic servomechanism (fig. 2). The ramp was designed so that the throat area in both ducts was varied simultaneously to allow inlet restarts and off-design Mach number operation.

Ejector bypass. - An ejector bypass was located in the bypass door cavity, as shown in figure 2. This bypass would permit airflow past the engine for cooling purposes when inlet-engine tests are conducted. The ejector bypass was sealed during this program.

Overboard bypass. - The overboard bypass system consisted of four slotted, sliding plate doors (the overboard exit of one can be seen in fig. 2). There were two doors for each duct. The doors were individually controllable by means of electrohydraulic servomechanisms. A typical closed-loop position response of one door is shown in figure 3. The bandwidth extends to about 110 hertz. The system was developed using the methods described in references 9 to 12. The basic purpose of the overboard bypass is to match inlet airflow to engine airflow. The two

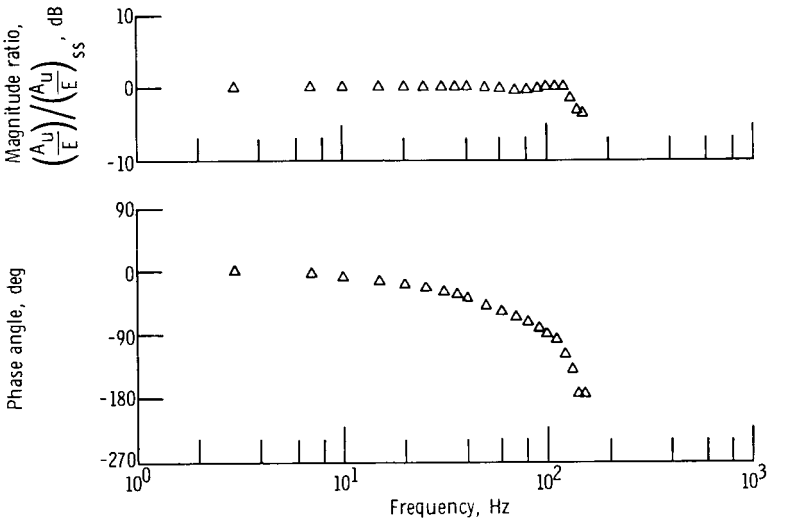

Figure 3. - Response of overboard bypass door to sinusoidal input voltage. Peak-to-peak movement, 0.42 centimeter (16 percent of maximum door travel).

doors in each duct were capable of bypassing approximately 88.5 percent of the duct airflow at the design Mach number. The overboard bypass door exits were choked. The bypass doors were also used during the investigation to produce airflow disturbances and as the variable to control terminal shock position.

Dynamic Instrumentation

Pressure transducers. - Static pressure measurements were made on the inlet cowl wall to determine shock position and for control feedback signals. The locations of the static taps are shown in figure 4. Each tap was closely connected to a strain-gage high-response pressure transducer. The frequency response of each

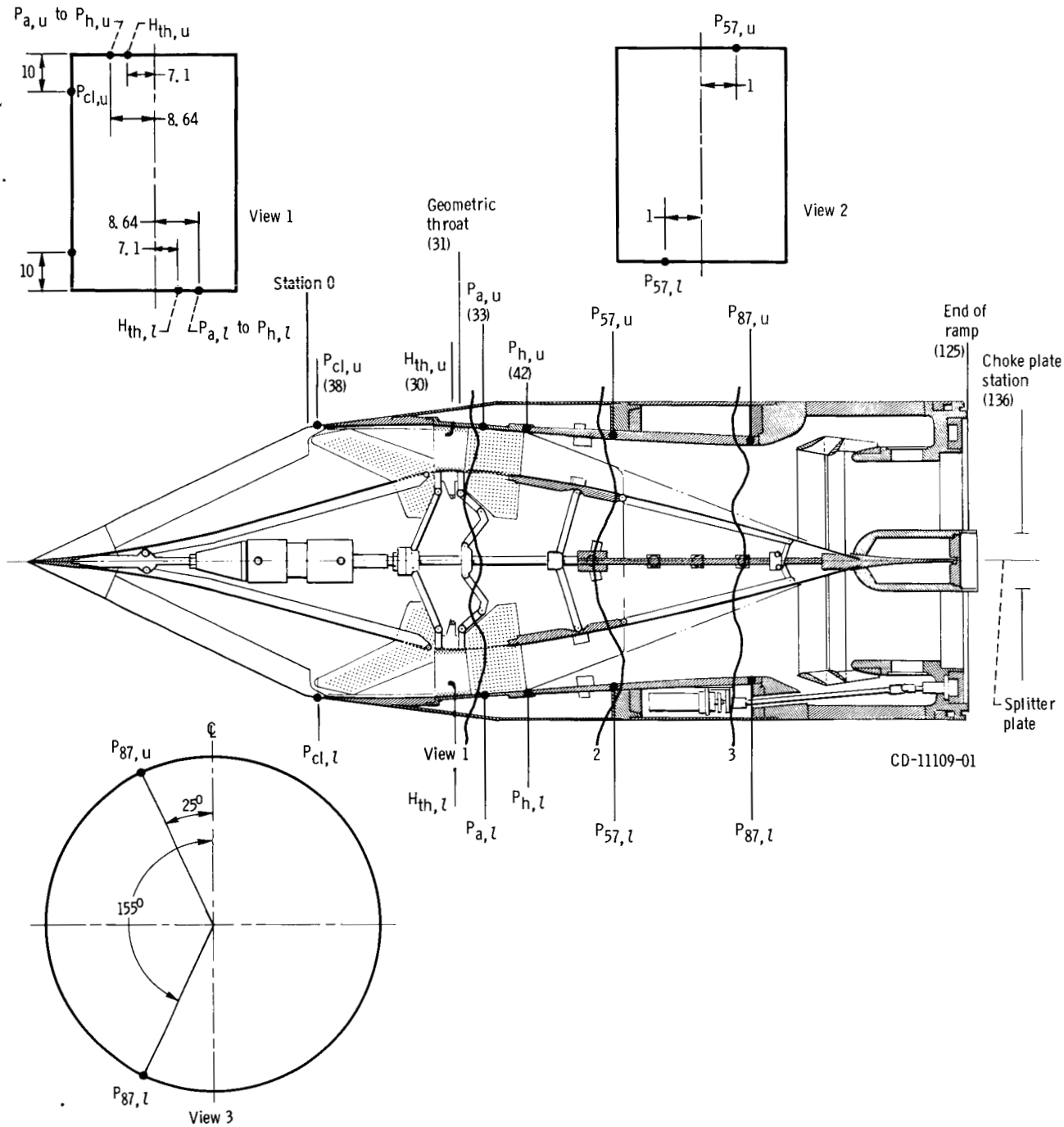

Figure 4. - Location of pressure transducers in upper and lower duct of two-dimensional inlet. Views 1, 2, and 3 show only inside cowl and/or sidewall surfaces, looking downstream. (Dimensions are in cm.)

pressure transducer and its connecting line was flat within 0 to +1 decibel and had less than 8° of phase lag in the frequency range of 0 to 200 hertz.

The cowl lip static pressure P_{cl} and the throat total pressure H_{th} (fig. 4) were also used as control signals. (Symbols are defined in the appendix.) Both pressures were connected to strain-gage-type dynamic pressure transducers. The ratio P_{cl}/H_{th} was used as an unstart signal to be described later.

The throat total pressure H_{th} was also used as the base for a reference signal for the electronic shock position sensor.

Electronic shock position sensor. - The eight throat static pressures (a to h) were used as inputs to a shock position sensor. The taps were equally spaced from a to h (fig. 4). The pressure at each tap was compared to a reference signal generated from the throat total pressure H_{th}. The shock was determined to be between the most upstream tap having a higher pressure than the reference and its adjacent upstream tap. Thus, the resolution of the sensor was limited by the tap spacing. The sensor had an electronic stepwise-continuous output proportional to shock position. A detailed discussion of the shock sensor is given in reference 7.

TEST PROCEDURE

The program was conducted in the 10- by 10-Foot Supersonic Wind Tunnel at the NASA Lewis Research Center. A desktop-size $\pm$10-volt analog computer, located in the wind tunnel control room, provided a versatile means for signal conditioning, programming controllers, and closing loops between controllers and the inlet bypass door and ramp servomechanisms.

Wind Tunnel Conditions

Terminal shock control and restart control system tests were conducted at a tunnel free-stream Mach number of 2.68. The corresponding free-stream conditions were total pressure, 9.55 newtons per square centimeter; total temperature, 320 K; specific heat ratio, 1.4; and test section Reynolds number, 7.75×10^{6} per meter.

Inlet Operating-Point Conditions

The following conditions were constant for all tests (both frequency response testing and unstart-restart transients): inlet pitch angle, 0°; and inlet diffuser

exit (choked orifice) corrected airflow, 14.2 kilograms per second.

The terminal shock operating point for all tests (unless otherwise noted) resulted in an average total pressure recovery of 0.88 at the compressor face station. This compares to a peak recovery for the inlet of about 0.93.

Prior to the experimental investigation it was intended to have the terminal shock operating point at the center of pressures taps a to h and to oscillate the shock over taps a to h. Because of a severe aerodynamic instability that occurred when the shock moved downstream of tap f, it was necessary to move the operating point forward somewhat. An open-loop peak-to-peak amplitude from a position upstream of tap a to a position between taps e and f was then used. The instability is discussed in the section INLET OPEN-LOOP CHARACTERISTICS.

Terminal Shock Control System Tests

The terminal shock control system was used as a regulator to maintain a commanded throat exit static pressure P_{57} or terminal shock position X_s while the inlet was subjected to bypass door area (and hence airflow) disturbances. The control performance was evaluated by frequency response testing. During these tests, one door in each duct was used to produce sinusoidal bypass door area disturbances in each duct of the inlet. The other door in each duct was used as the manipulated variable of the terminal shock controller.

Frequency response testing of the terminal shock control system was accomplished as follows: With the shock control loop open, a peak-to-peak shock displacement of about 9.5 centimeters was set up as a result of a change in disturbance bypass door area. A bypass disturbance of ± 16 square centimeters was required to produce this amplitude of shock displacement. This area disturbance is equivalent to a corrected airflow disturbance of approximately ± 0.38 kilogram per second, or ± 2.7 percent of the diffuser exit (choke plate) corrected airflow. Steady-state data were then obtained at the shock operating point and at the peak upstream and downstream positions of the oscillation. The shock position control loop was then closed, and responses were taken for disturbance frequencies of 1 to 150 hertz. The throat exit static pressure P_{57} was used as the signal for evaluating performance because it was continuous whereas the shock sensor had discrete output levels. The responses were measured on line by means of a commercially available frequency response analyzer. The data are presented as plots of amplitude ratio against disturbance frequency.

The amplitude ratio plotted in all cases is P_{57}/A_d and is normalized to the steady-state open-loop value of the amplitude ratio. The ideal control would have an amplitude ratio of zero at all disturbance frequencies. Since this is not possible, it is desirable to have the smallest amplitudes possible over the test frequency range.

Restart Control System Tests

In all cases the inlet was unstarted by a decrease in overboard bypass door airflow. This was accomplished in one of two ways. One method used one door for disturbance and one for control in each duct. The unstart was accomplished by applying a step command in the closed direction to the disturbance door position servomechanism. Unstart from the usual terminal shock operating point could not be achieved by this method because the shock control system was fast enough to prevent it. Thus, for this method to work, the terminal shock had to be initially placed at the verge of unstart (approximately at the geometric throat). The other method of unstart was to use both doors in each duct for control and to pulse the terminal shock controller setpoint so as to close the bypass doors. (Both doors were needed to achieve the necessary flow disturbance.) This allowed the inlet to be unstarted from the usual terminal shock operating position (0.88 total pressure recovery). When unstart was sensed, the setpoint pulse was automatically removed.

Inlet unstart-restart transients were evaluated by monitoring various inlet aerodynamic and variable geometry position feedback signals during the transient. These data were recorded on a 14-channel FM tape recorder for evaluation after the program.

INLET OPEN-LOOP CHARACTERISTICS

Three signals of interest for feedback in terminal shock controls are terminal shock position X_s, throat exit static pressure P_{57}, and diffuser exit static pressure P_{87}. Terminal shock position is of particular interest because it is the variable being controlled. Because of the difficulty of measuring actual shock position, it is often measured indirectly or inferred from a throat static pressure measurement downstream of, but near, the terminal shock (refs. 2 and 3). Use of the diffuser exit pressure as a second feedback signal significantly improved terminal shock control (ref. 3). The reason for this is that the delay time resulting from the pressure wave traveling up the duct between the disturbance and the diffuser exit pressure is shorter than that between the disturbance and the throat pressure.

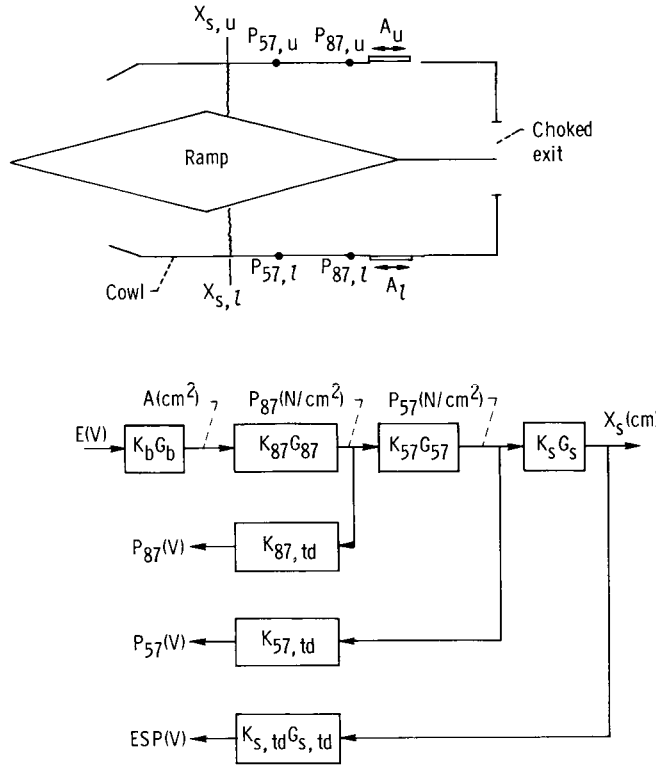

Figure 5. - Block diagram of inlet signals.

A signal flow block diagram of the inlet showing the various signals measured and the definitions of the transfer functions between these signals is presented in figure 5. The K factors represent the steady-state gains of the transfer functions, and the G factors represent the dynamic terms (the frequency-dependent part) of the transfer functions. The pressure transducer dynamics were independent of frequency (i.e., G = 1) for the frequency range of interest in this report. This was not the case for the shock position sensor.

Inlet Steady-State Gains

The inlet steady-state gains of upper-duct signals - shock position $X_{s,u}$ and static pressures $P_{57,u}$ and $P_{87,u}$ - to an upper-duct bypass door area disturbance $A_{d,u}$ are given in table I for a free-stream Mach number of 2.7. These gains, which were the same for lower-duct signals to a lower-duct disturbance, represent typical values for the terminal shock operating-point condition chosen. Reference 6 shows that the steady-state changes in lower-duct signals due to an upper-duct

TABLE I. - STEADY-STATE GAINS OF INLET SIGNALS

[Free-stream Mach number, 2.7.]

Steady-state gain	Ratio of variables
$K_{87}K_{57}K_s$	$X_{s,u}/A_{d,u} = 0.297$ cm/cm^2
$K_{87}K_{57}$	$P_{57,u}/A_{d,u} = 0.026$ N/cm^2/cm^2
K_{87}	$P_{87,u}/A_{d,u} = 0.016$ N/cm^2/cm^2

disturbance were only 20 percent (or less) of the change in the equivalent upper-duct signal (e.g., $(X_{s,\ell}/A_{d,u})/(X_{s,u}/A_{d,u}) = 0.2$).

Inlet Dynamics

For comparison, some of the open-loop inlet dynamic responses from reference 6 are repeated here. They describe the plant that is to be controlled as a reference for the closed-loop data. The data presented are the frequency-dependent part of the dynamics only (the G factors of fig. 5). The data presented are for the response of upper-duct signals to an upper-duct bypass door area disturbance. Reference 6 indicates that the responses of the lower-duct signals to a lower-duct disturbance were the same. Although the data are not repeated here, reference 6 shows that the gain of a lower-duct signal to the equivalently located upper-duct signal (e.g., $X_{s,\ell}/X_{s,u}$) decreases rapidly with frequency (from 0.2 or less at 0 Hz to 0.05 or less at 25 Hz) when a disturbance occurs in the upper duct.

Shock position dynamics. - In terms of the block diagram of figure 5 the transfer function relating the shock position sensor output to a bypass door area disturbance is

$$\frac{ESP_u}{A_{d,u}} = K_{87}G_{87}K_{57}G_{57}K_sG_sK_{s,td}G_{s,td}$$

With the steady-state gain terms removed the response is

$$\left(\frac{ESP_u}{A_{d,u}}\right) \Bigg/ \left(\frac{ESP_u}{A_{d,u}}\right)_{ss} = G_{87}G_{57}G_sG_{s,td}$$

and is referred to in this report as the normalized open-loop frequency response. The normalized shock position response for a Mach number of 2.7 is plotted in figure 6(a). The amplitude response shows that shock amplitude is 3 decibels or more

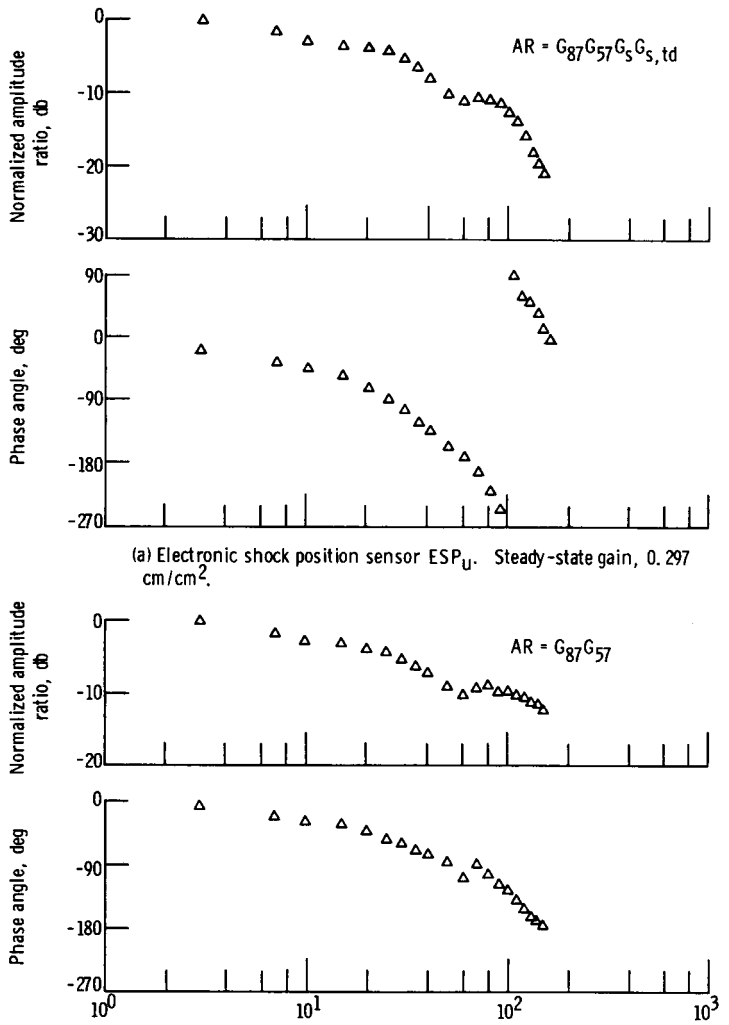

(a) Electronic shock position sensor ESP_u. Steady-state gain, 0.297 cm/cm^2.

(b) Throat exit static pressure $P_{57,u}$. Steady-state gain, 0.026 $N/cm^2/cm^2$.

Figure 6. - Frequency responses of upper-duct signals to upper-duct bypass door disturbances. Mach 2.7; angle of attack, 0^0; back-pressured bleeds.

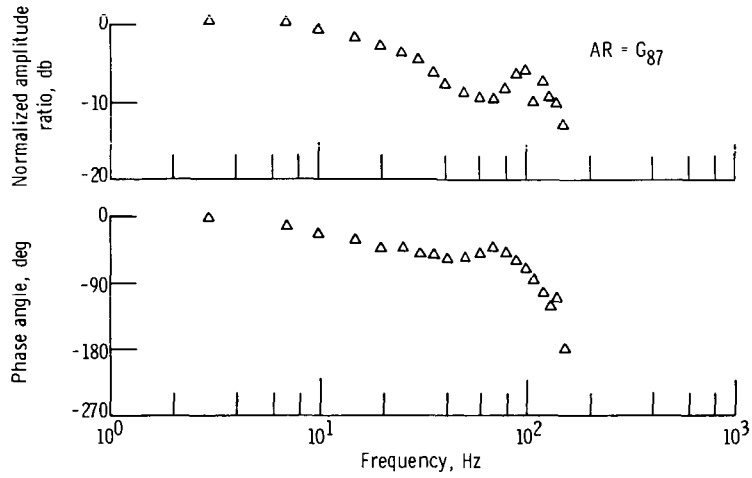

(c) Diffuser exit static pressure $P_{87,u}$. Steady-state gain, 0.016 $N/cm^2/cm^2$.

Figure 6. - Concluded.

down from its 1-hertz disturbance amplitude at frequencies of 10 hertz and above. Phase lag is about 45^o at 10 hertz and increases to 180^o at about 60 hertz.

Throat exit static pressure dynamics. - The transfer function relating the measured throat exit static pressure $K_{57,td}P_{57,u}$ to a bypass door area disturbance is (fig. 5)

$$\frac{K_{57,td}P_{57,u}}{A_{d,u}} = K_{87}G_{87}K_{57}G_{57}K_{57,td}$$

The normalized response is

$$\left(\frac{P_{57,u}}{A_{d,u}}\right) \Bigg/ \left(\frac{P_{57,u}}{A_{d,u}}\right)_{ss} = G_{87}G_{57}$$

The normalized throat exit static pressure response is shown in figure 6(b). The amplitude response is 3 decibels or more down from its 1-hertz disturbance ampli-

tude at frequencies of 10 hertz and above. Phase lag is about 30° at 10 hertz and increases to 180° at about 150 hertz. Thus, as expected, the throat pressure exhibits less phase lag than shock position.

Diffuser exit static pressure dynamics. - The transfer function relating the measured diffuser exit static pressure $K_{87,td}P_{87,u}$ (fig. 5) to a bypass door area disturbance is

$$\frac{K_{87,td}P_{87,u}}{A_{d,u}} = K_{87}G_{87}K_{87,td}$$

The normalized response is

$$\left(\frac{P_{87,u}}{A_{d,u}}\right) \Bigg/ \left(\frac{P_{87,u}}{A_{d,u}}\right)_{ss} = G_{87}$$

and the experimental results are given in figure 6(c). The diffuser exit pressure is 3 decibels or more down from its 1-hertz disturbance amplitude at frequencies of about 20 hertz and above. Phase lag is about 45° at 20 hertz and increases to 120° at 130 hertz. Since the diffuser exit pressure is the closest of the three signals to the disturbance, it exhibits the least amount of phase lag in response to the bypass door disturbance.

Inlet Instability

Early in the experimental program an inlet instability was found to occur as the shock was moved downstream of the inlet throat by increasing bypass door area. The severity of the instability seemed to increase as the shock operating point moved progressively farther downstream. The effect of the instability on pressures throughout the inlet is indicated in figure 7. This figure shows traces of several pressures in the inlet's upper duct. At the beginning of the traces the doors are nearly closed and the terminal shock is forward of tap $P_{a,u}$. As the doors begin to ramp open the terminal shock moves downstream. This is indicated in the traces by decreasing pressure. As the shock approaches the pressure tap $P_{a,u}$ the noise levels of all the pressure signals begin to increase. At one point the $P_{a,u}$ pressure

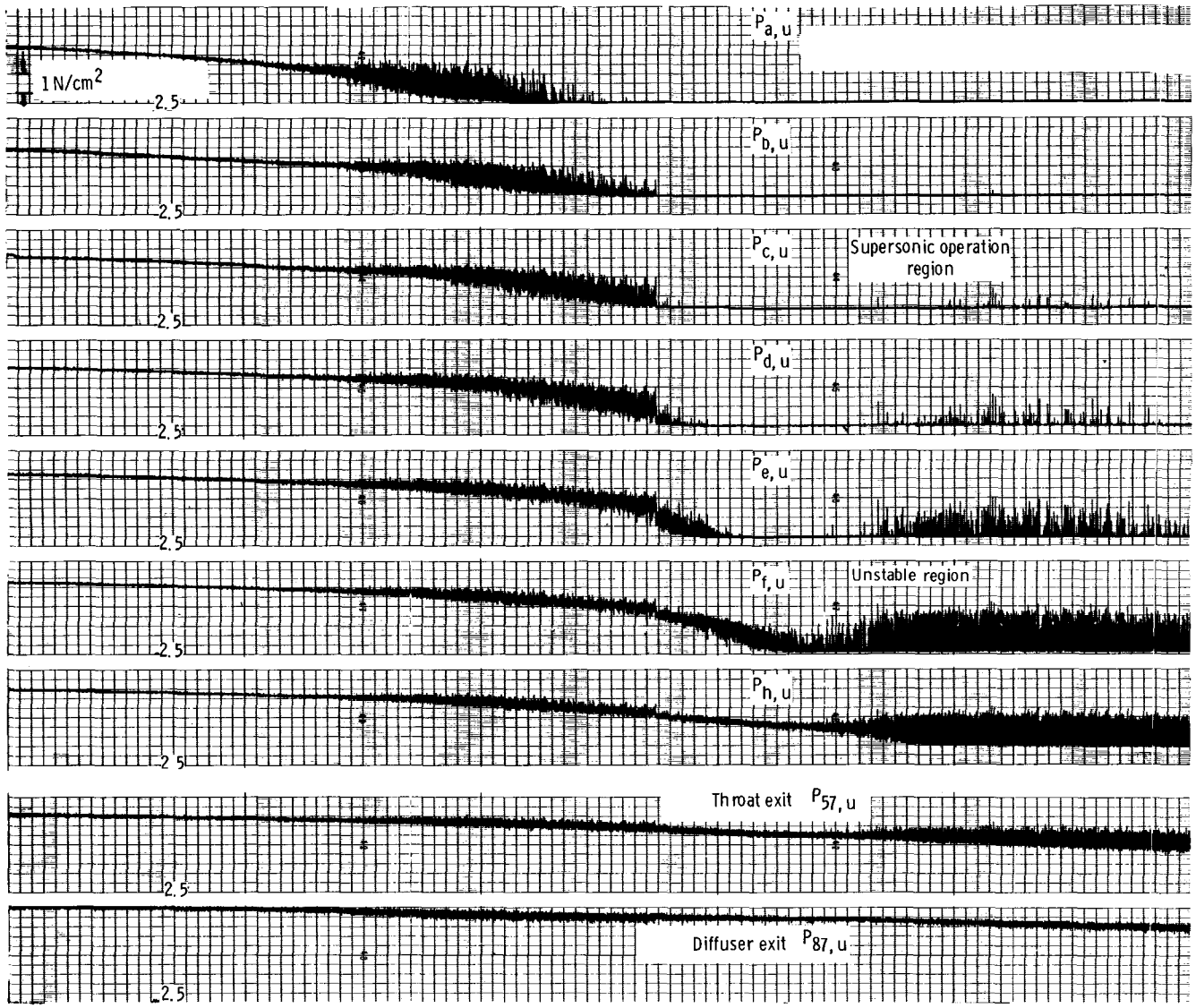

Figure 7. - Static pressure changes as terminal shock traverses inlet. (Vertical scale of each trace begins at 2.5 N/cm^2.)

level rises and falls rapidly (found to be about 30 Hz from faster traces not shown) between its supersonic (low) pressure level and a subsonic (high) pressure level. The shock appears to oscillate over one tap only until the shock moves aft of tap $P_{f,u}$. The instability then increases significantly in amplitude (and frequency increases to about 50 Hz) and can be seen to propagate from downstream of tap $P_{h,u}$ to upstream of tap $P_{c,u}$ and even to $P_{b,u}$ at one point.

The instability is thought to result from a local flow angle discontinuity where the cowl corners initially begin the transition from rectangular to round. This transition begins at about the same station as the $P_{h,u}$ tap location. It is believed that when the shock approaches the discontinuity a boundary-layer thickening occurs which causes the instability. Also when the terminal shock moves downstream of the transition region, shocks may be generated by the transition corners, helping to trigger the instability and increasing its severity.

As can be seen from figure 7 the instability resulted in noise-contaminated feedback signals. The noise on these signals was far worse than that encountered in the axisymmetric inlet tests reported in reference 3. The relative noise levels of the P_{57} and P_{87} signals as a function of frequency are shown in figure 8. As shown, the signals contained high noise levels at frequencies other than the disturbance frequency. When the disturbance frequency is 140 hertz, the noise spectra of the inlet signals do not clearly reveal the presence of the disturbance signal.

Although the instability resulted in feedback signals that were severely contaminated with noise, it was decided to continue the control investigation to determine types of terminal shock control that would perform reasonably well in spite of

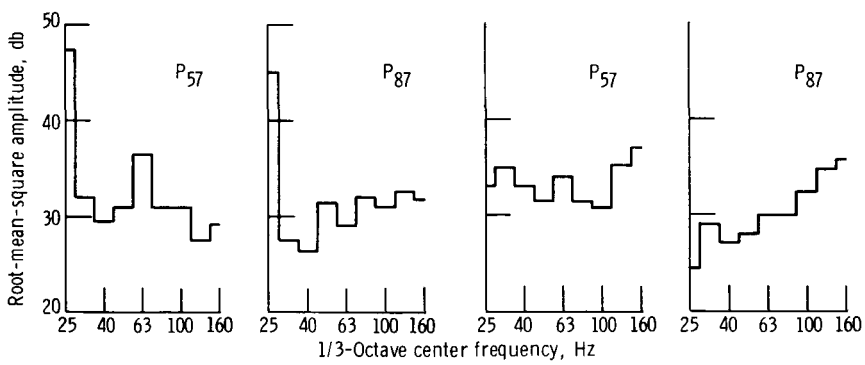

(a) Disturbance frequency, 25 hertz. (b) Disturbance frequency, 140 hertz.

Figure 8. - Noise spectrums of inlet signals without control at two different bypass door disturbance frequencies.

the noise problem. The noise problem caused mechanical problems with the control bypass door hardware. This ultimately resulted in the definition of a control system performance criterion which included not only how well shock motion is attenuated, but also bypass door response to signal noise as a penalty. This is discussed in a later section.

RESULTS AND DISCUSSION

Terminal Shock Control Systems

The terminal shock control systems that were tested are shown in block diagram form in figure 9.

Figure 9(a) shows the case where pressure signals were used for feedback. All blocks have been previously defined except for $K_{c57}G_{c57}$ and $K_{c87}G_{c87}$, which represent the P_{57} and P_{87} controller transfer functions, respectively. One- and

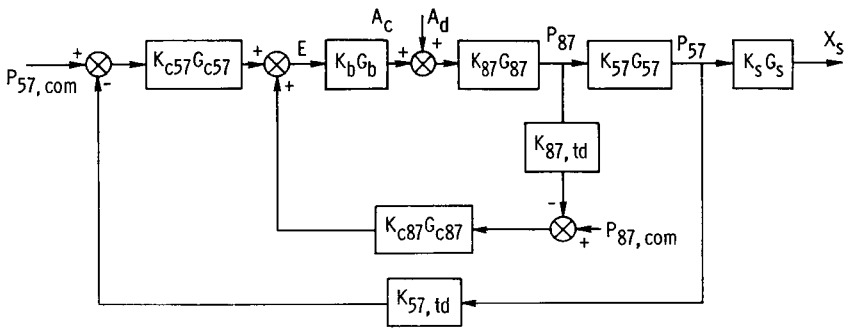

(a) Throat exit P_{57} and/or diffuser exit P_{87} pressure feedback.

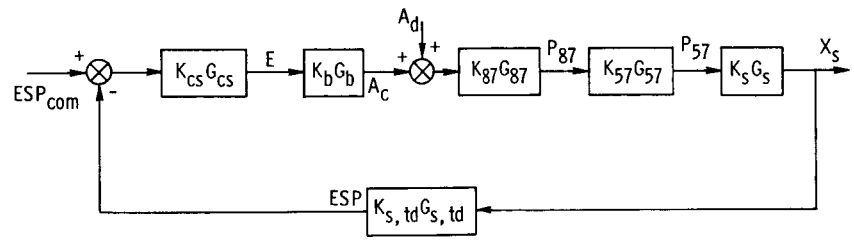

(b) Shock position sensor (ESP) feedback.

Figure 9. - Block diagram of terminal shock control system using either throat exit static P_{57} and/or diffuser exit static P_{87} pressure feedback or electronic shock position sensor output ESP feedback.

two-loop pressure feedback controls were tested using P_{57} and/or P_{87} feedback.

Figure 9(b) shows the case where the output of the electronic shock sensor was used for feedback. The only block not previously defined is $K_{cs}G_{cs}$, which represents the shock position controller transfer function.

As is indicated in the INTRODUCTION, one potential problem relative to controlling the two-dimensional inlet could have resulted from the airflow coupling that exists between the inlet's two ducts. Although the coupling was found to be small (see section INLET OPEN-LOOP CHARACTERISTICS), a test was conducted in which each duct was controlled independently. A disturbance was introduced in the upper duct only and $P_{57,u}$ and $P_{57,l}$ responses were taken. The resulting disturbance in $P_{57,l}$ was so small as to be almost unmeasurable. No interactions between the control systems were noted, and it was assumed in subsequent terminal shock control tests that the ducts could be controlled independently. Therefore, only results for the upper duct will be shown and the u subscript will be dropped. If the coupling had been substantial, it would probably be necessary to have a single controller for both ducts or some sort of coupling between the two duct controllers. Since both ducts of the inlet feed a single engine, it may be desirable to have some controller coupling in any case. Thus, it might be possible to minimize compressor face distortion that results from such things as sideslip or an unstart of only one duct.

Single-loop control. - One objective of the controls program was to obtain a two-loop control that was an improvement over that reported in reference 3. Therefore, possible single-loop controls which could be used in the two-loop control were tested first. These consisted of a proportional-plus-integral-type control with either P_{57} or shock sensor output feedback and a proportional control with P_{87} feedback.

Proportional-plus-integral control using throat static pressure P_{57} feedback: This control system is shown in figure 9(a) where $K_{c87}G_{c87} = 0$ and $K_{c57}G_{c57}$ is of the form $K_{c57}[(s/\omega_c + 1)]/s$ (s being the Laplace variable).

The amplitude frequency response for two different values of ω_c and slightly different loop gains are shown in figure 10(a). The amplitude ratio in terms of transfer functions of figure 9 is indicated in the figure. An ideal control would have an amplitude ratio of zero for all disturbance frequencies. Since this is not possible, the smaller the amplitude ratio the controlled system has, the better its performance. The controller with an ω_c of 157 radians per second (25 Hz) has amplitudes below that with an ω_c of 628 radians per second (100 Hz) over the frequency range

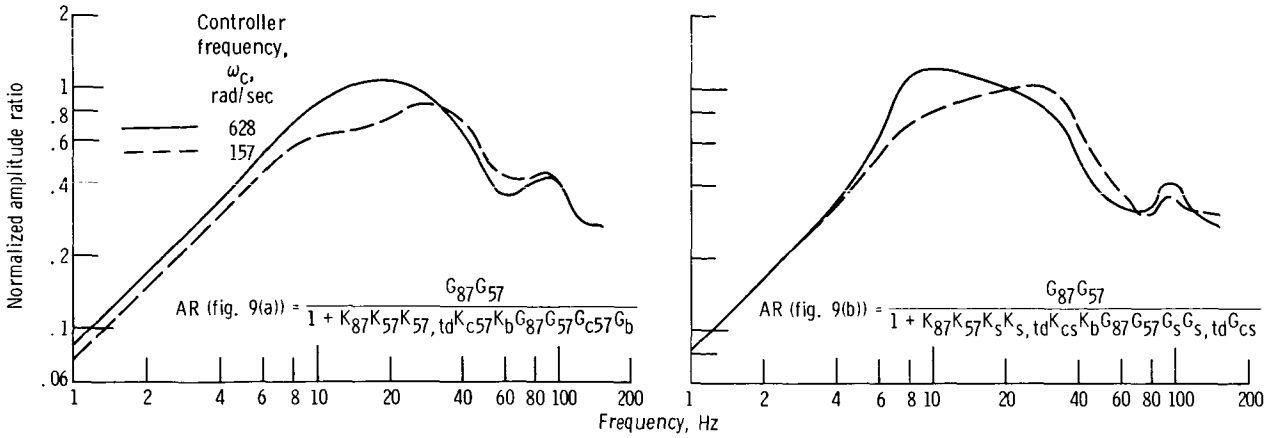

(a) P_{57} feedback.

(b) ESP feedback.

Figure 10. - Closed-loop frequency response of throat exit static pressure P_{57} to bypass door disturbance for single-loop proportional-plus-integral controller using either P_{57} or electronic shock position sensor ESP feedback for different values of controller parameters. $G_{cs} = G_{c57} = [(s/\omega_c) + 1]/s$.

of 1 to 30 hertz. The better response probably results from less controller phase lag in the lower frequency region. Between 30 and 90 hertz the control response with an ω_c of 157 radians per second (25 Hz) was somewhat worse.

Proportional-plus-integral control using electronic shock position sensor (ESP) feedback: The block diagram for this control system is shown in figure 9(b). The amplitude frequency responses for proportional-plus-integral control using the shock sensor output for feedback are shown in figure 10(b). The two curves are for different values of ω_c. The loop gains were the same. As was the case with P_{57} feedback the controller with the smaller value of ω_c had a better response in the low-frequency range (4 to 20 Hz). And the response was somewhat worse between 20 and 70 hertz.

Comparison of proportional-plus-integral control using throat static pressure P_{57} or electronic shock position sensor (ESP) output feedback: Frequency responses of P_{57} to bypass door disturbance using proportional-plus-integral control and with either P_{57} or electronic shock sensor feedback are compared in figure 11. The response for the uncontrolled inlet is also shown. The value of ω_c was the same for both cases (157 rad/sec). The loop gain was about 1.13 times higher for the control using P_{57} feedback. The control using P_{57} feedback appears to be somewhat better as it resulted in greater attenuation over the 1- to 40-hertz frequency range. Increasing the controller gain for the shock sensor feedback control

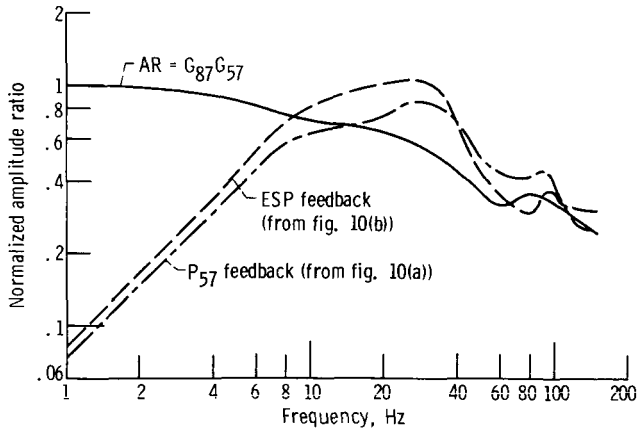

Figure 11. - Comparison of open- and closed-loop throat exit static pressure P_{57} response to bypass door disturbance. Single-loop proportional-plus-integral controller using either P_{57} or electronic shock position sensor ESP feedback. $G_{c57} = G_{cs} = [(s/157) + 1]/s$.

to match the P_{57} feedback loop gain would probably result in the same responses for the two cases in the 1- to 5-hertz range. But the shock sensor feedback control would become more resonant in the higher frequency regions (25 to 30 Hz and 90 Hz). The resonance with the P_{57} feedback is lower because it has less phase lag than shock position in response to bypass door disturbances (at 30 Hz, P_{57} is 62° compared to 109° for shock position). But there is not a substantial degradation in control dynamic performance using shock feedback (as compared to P_{57}). An advantage of shock position feedback is that the variable being controlled is being measured directly. Thus, it might be possible to eliminate the need for scheduling of the feedback variable as a function of flight conditions (e.g., Mach number, inlet geometry, etc.).

Proportional control using diffuser exit static pressure P_{87} feedback: Inlet control using diffuser exit static pressure P_{87} in a proportional feedback loop was tried. The block diagram for this control is shown in figure 9(a) where $K_{c57}G_{c57} = 0$ and $G_{c87} = 1$. The results are shown in figure 12. The solid curve represents the uncontrolled inlet response, and the dashed curve is the response with control. Attenuation in P_{57} below open-loop values occurred to a frequency of about 25 hertz, whereas the best single-loop P_{57} feedback proportional-plus-integral control attenuated shock position below open-loop values out to 15 hertz (fig. 11). Because the P_{87} signal is located closer to the disturbance, it has less phase lag

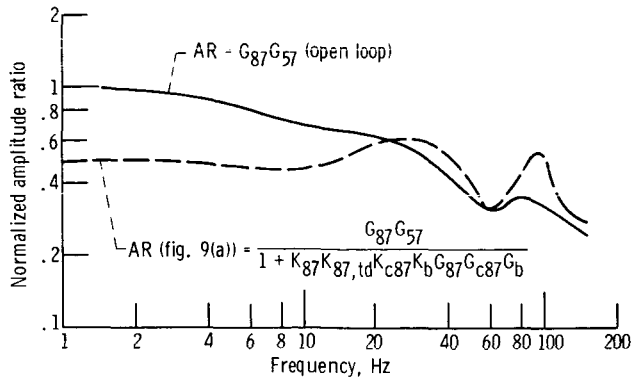

Figure 12. - Comparison of open- and closed-loop throat exit static pressure P_{57} response to bypass door disturbance. Single-loop proportional controller using diffuser exit static pressure P_{87} feedback. $G_{c87} = 1$.

than P_{57} or shock position. As is shown in reference 3, it thus provides improved control performance in the mid-frequency range. Analysis prior to the experimental investigation indicated that the addition of lead-lag compensation with a predominate lead would help to improve the control response further. This was precluded, however, because of signal noise problems caused by the shock instability. This is discussed in greater detail later (in the section Control System Noise Problem).

Two-loop control. - The two-loop control system of figure 9(a) was tested next. The proportional controller using P_{87} feedback was the same one as that used for the test of figure 12. The proportional-plus-integral controller using P_{57} feedback was the same one as that used for the test of figure 10(a) (ω_c = 628 rad/sec). The response of this system compared to that of the uncontrolled system and that of the single-loop proportional-plus-integral control system is shown in figure 13. The addition of the proportional loop improved the closed-loop response of the system relative to the single-loop proportional-plus-integral control by achieving attenuation below the open loop out to 20 hertz as compared to 7 hertz. Relative to the single-loop control (fig. 10(a), ω_c = 628 rad/sec) the two-loop response shows greater attenuation than the single-loop response out to a frequency of 30 hertz; between 30 and 80 hertz the two responses are similar; between 80 and 110 hertz the two-loop response is more resonant than that of the single loop.

Thus, on a frequency response basis the two-loop control appears to provide a substantial improvement over the single-loop control. However, the addition of the proportional diffuser exit static pressure loop resulted in noise being propagated in

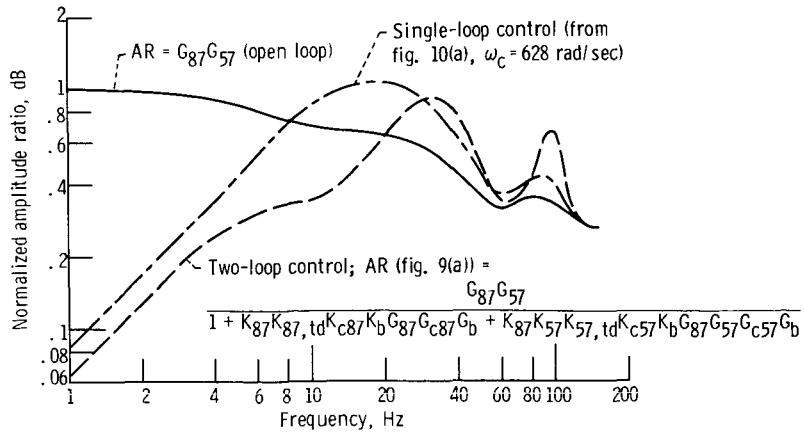

Figure 13. - Comparison of open- and closed-loop throat exit static pressure P_{57} responses to bypass door disturbances - two-loop and single-loop controls. Two-loop control: Proportional-plus-integral controller using P_{57} feedback and proportional controller using P_{87} feedback; single-loop control: proportional-plus-integral controller using P_{57} feedback; $G_{c57} = [(s/628) + 1]/s$ for both cases; $G_{c87} = 1$.

the closed-loop system, which caused bypass door mechanical problems. Because of this problem no further attempt was made to investigate two-loop controls. This problem, which was not encountered to a serious degree in the axisymmetric inlet controls program (ref. 3), is discussed in the next section.

Control System Noise Problem

The increase in unwanted control door activity due to the addition of the proportional control loop is demonstrated in figure 14, which shows traces of disturbance and control bypass door feedback voltages for controls with and without the proportional loop. The outer loop proportional-plus-integral controller was the same for both cases, $100[(s/628) + 1]/s$, and used P_{57} feedback. The two-loop controller used proportional P_{87} feedback and had the same loop gains as for the case shown in figure 13.

The traces of figure 14 show the disturbance bypass doors oscillating at a frequency of 1 hertz with a peak-to-peak amplitude of about 0.42 centimeter for both cases. And in both cases the control bypass doors are shown to be responding with high-frequency oscillations superimposed on a basic 1-hertz peak-to-peak amplitude of 0.35 centimeter. Without the proportional control loop, the largest control door peak-to-peak amplitude due to noise is about 0.18 centimeter (fig. 14(a)). With the proportional loop there are frequent control door peak-to-peak amplitudes as large

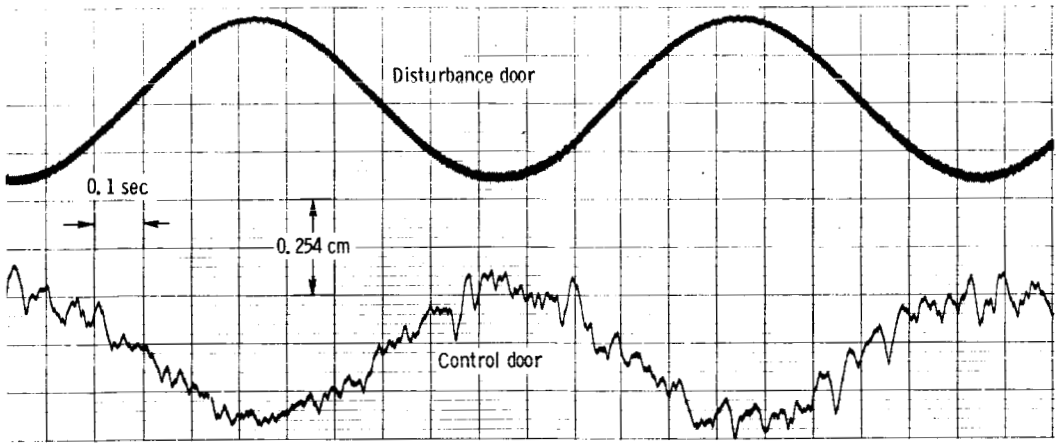

(a) Without proportional loop.

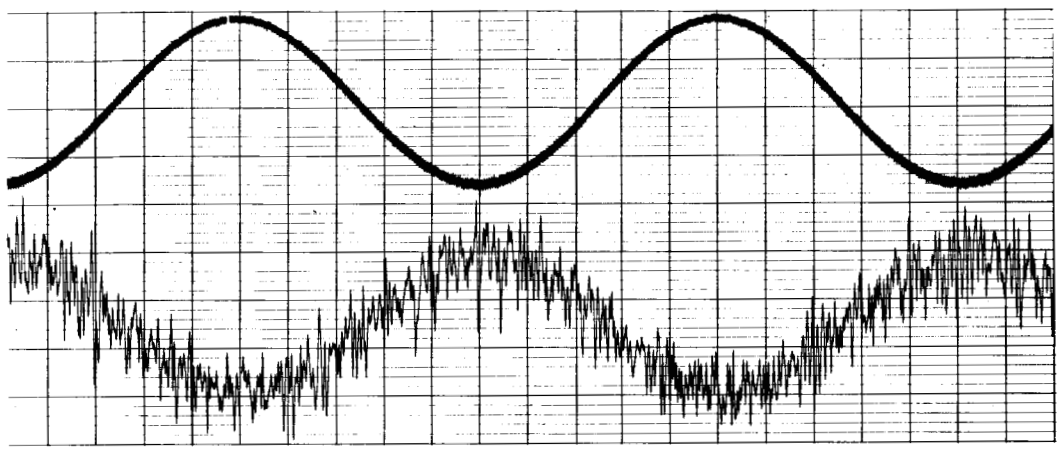

(b) With proportional loop.

Figure 14. - Comparison of control bypass door position feedback voltage with and without proportional diffuser exit static pressure P_{87} feedback loop. Disturbance bypass door frequency, 1 hertz.

as 0.35 centimeter (fig. 14(b)). In general the control door activity due to noise is increased greatly by the addition of the proportional loop to the control system.

The frequency content of the control door noise for the two cases (1-Hz disturbance) was analyzed by a commercially available 1/3-octave noise analyzer. The results are shown in figure 15. (The center frequency of the lowest 1/3-octave bandpass filter that was available was 25 Hz.) As expected, figure 15 shows the control door amplitudes to be much greater in the two-loop case than in the single-loop case. In the two-loop case the control doors show peaks at about 30 and 100 hertz (corresponding to the resonance points of fig. 13). In the single-loop case the control door amplitude peaks at 25 hertz and then decreases with frequency. For comparison

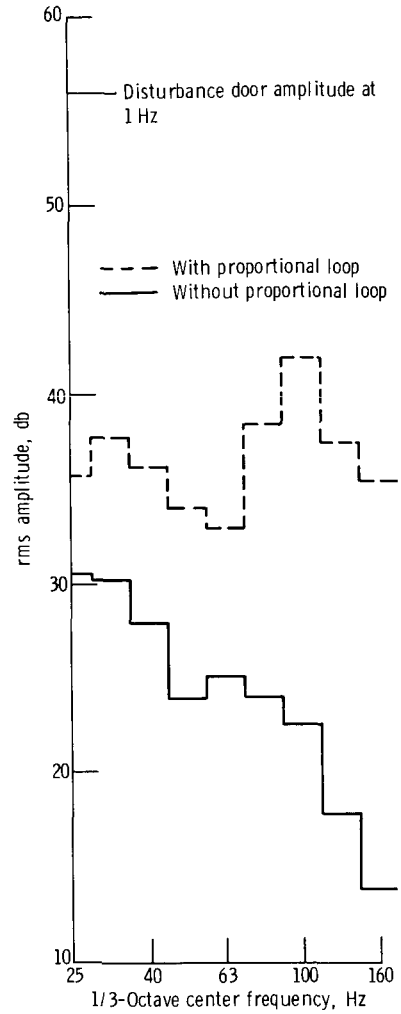

Figure 15. - Comparison of control bypass door noise frequency content with and without proportional diffuser exit static pressure P_{87} feedback loop. Disturbance bypass door frequency, 1 hertz.

purposes, the disturbance door amplitude is indicated on the edge of the decibel scale.

The control door noise problem is a direct result of the addition of the proportional inner loop. This can easily be demonstrated with the aid of figure 16. The figure shows controller voltage output per newton per square centimeter of error input as a function of frequency. As can be seen from figure 16, the proportional-plus-integral controller gain decreases as frequency increases to 100 hertz. Beyond

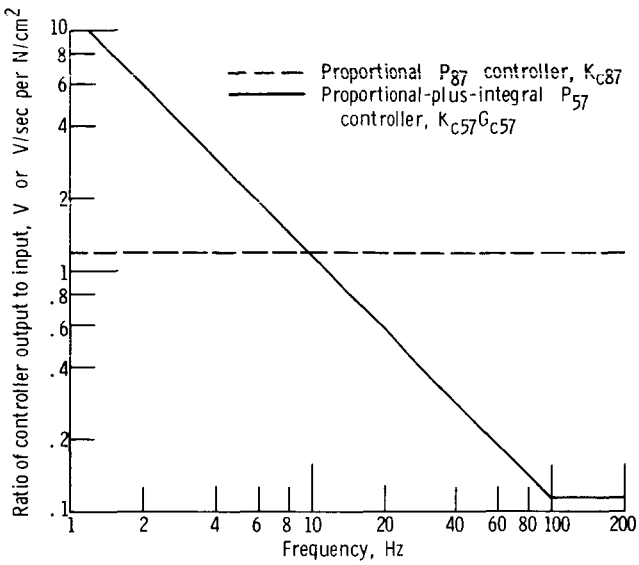

Figure 16. - Comparison of proportional and proportional-plus-integral controller output to input ratios as function of frequency. (Input of 1 N/cm^2 = 0.725 V for both controllers.)

100 hertz, the gain is constant. The proportional controller gain is, of course, constant over the entire frequency range.

Figure 8 showed the noise spectra of P_{57} and P_{87} to be about the same and to have fairly constant levels over the frequency range shown. Thus, when the control loops are closed and when there are no, or only low-frequency, airflow disturbances going on, the single-loop controller filters out the unwanted noise frequencies. Therefore, the unwanted control door activity due to noise decreases over the noise spectrum. The two-loop control, by virtue of the proportional inner loop, propagates considerably more noise to the control doors. For example, at 100 hertz the proportional loop has 10 times the gain of the proportional-plus-integral loop (fig. 16), which results in a much higher level of unwanted activity. Beyond 100 hertz, the bypass door response drops off rapidly, which accounts for the rapid dropoff of door activity in that frequency range (fig. 15).

This noise problem is serious and would be unacceptable in a flight application. Three failures occurred during the wind tunnel program which probably can be attributed to this problem. Control door actuators failed in two instances, and there was a hydraulic line fatigue failure in the other. One way to minimize or reduce the unwanted bypass door activity due to signal noise is to choose the controller parameters in a suitable manner. Such a possibility is discussed in the next section.

Optimization of Controller Parameters to Minimize Signal Noise Problems

The problem of unwanted signal noise lends itself nicely to system optimization analysis. There has been an effort at Lewis, such as that reported in reference 13, which deals with this subject. Basically, a performance index must be chosen which indicates how well the system performs. Then an optimum controller is determined that minimizes the performance index.

At the time of the wind tunnel program an analytical effort was underway to develop a digital computer program which would find the optimum controller parameters for a suboptimal controller structure such as proportional-plus-integral. The program was not completed in time for use during the experimental program. However, some studies were made after completion of the experimental program, and a typical result is shown in figure 17. In this case the computer program was applied to the inlet problem to determine the optimum controller parameters for a proportional-plus-integral controller using P_{57} feedback. The controller transfer function was

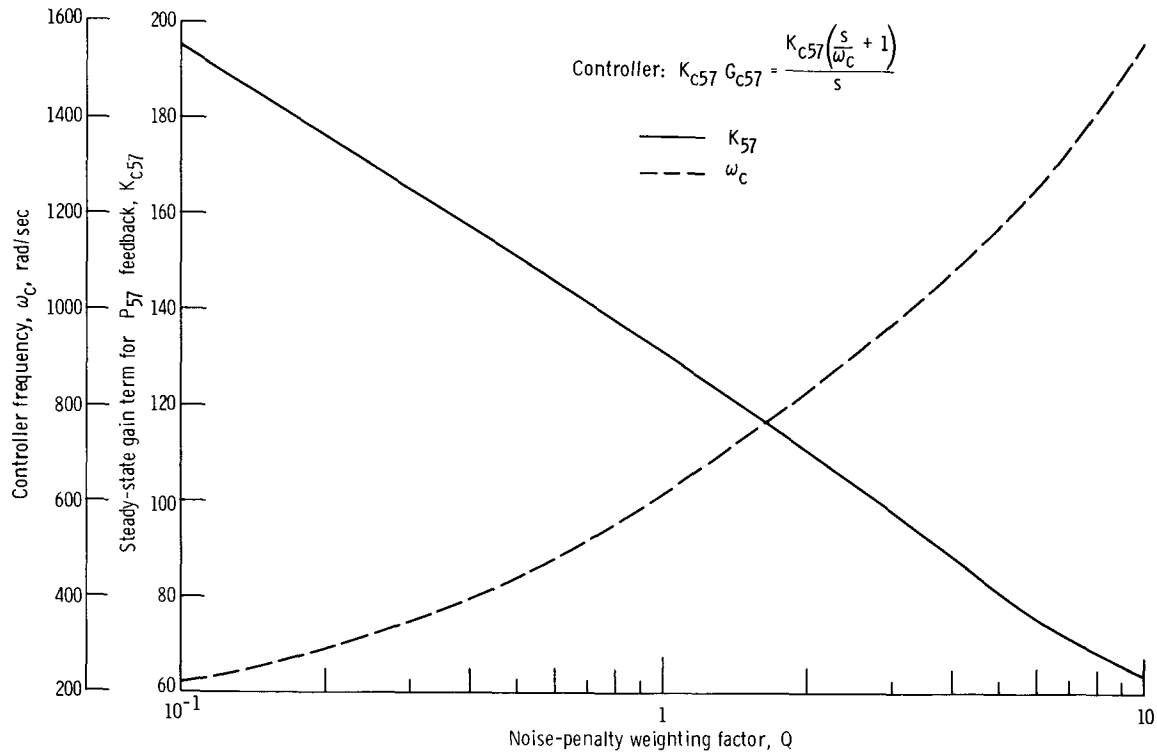

Figure 17. - Optimum values of controller parameters as functions of relative noise-penalty weighting factor.

$$K_{c57}G_{c57} = \frac{K_{c57}\left(\frac{s}{\omega_c} + 1\right)}{s}$$

The performance index consisted of two terms - the mean square regulation error in P_{57} and the control door kinetic energy due to signal noise. The optimum values of K_{c57} and ω_c are plotted as a function of noise-penalty weighting factor Q. As expected, figure 18 shows that, as the bypass door activity due to noise is penalized more heavily by increasing Q, K_{c57} decreases and ω_c increases. A combination of engineering judgment of experimental results (how much unwanted control door activity is acceptable) plus some analytical results (such as fig. 17) can be used to find the optimum values of K_{c57} and ω_c. This method also provides a much simpler and quicker means of arriving at controller parameters than do the classical methods (such as root locus) that were used in reference 3.

Restart Control System

A diagram of the restart control system is shown in figure 18. Each duct had an unstart sensor which used the ratio of a sidewall static pressure near the cowl lip

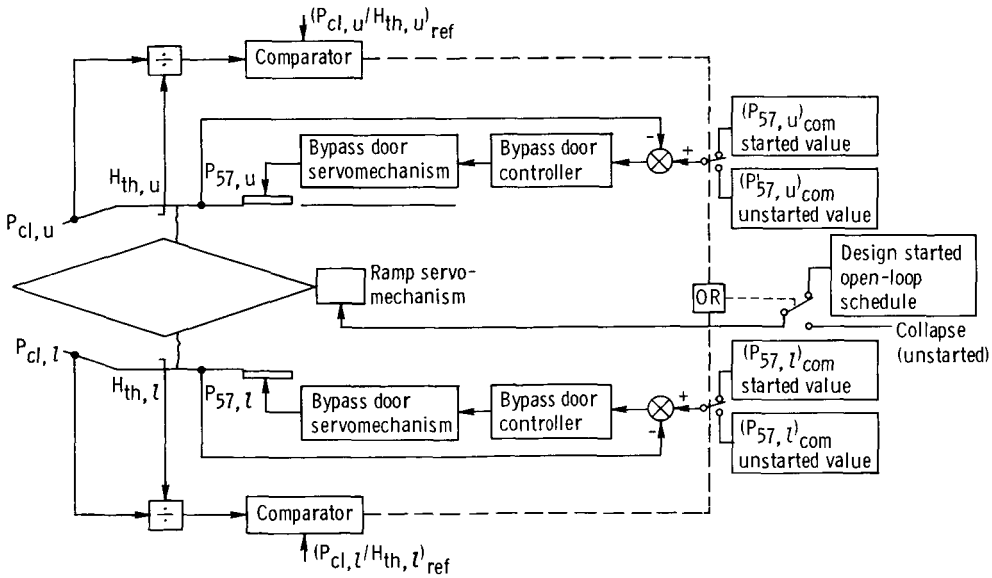

Figure 18. - Restart control system schematic.

P_{cl} (fig. 4) to a throat total pressure H_{th}. This pressure ratio is high when the inlet is unstarted because the cowl static pressure is in a subsonic flow region (high pressure) and inlet total pressure recovery is low. For started conditions the ratio is low since the cowl static pressure is in a supersonic (low pressure) region and total pressure recovery is high. Thus, a started or unstarted inlet condition can be detected by comparing the ratio to the proper reference level. The outputs of the unstart comparators were input to an OR gate which controlled the centerbody (ramp) position command. If an unstart was detected in either duct, the ramp was commanded to collapse, thereby increasing the ratio of throat- to capture-flow area in both ducts until both ducts were started. Then the ramp was commanded to return to design position. During these tests the design ramp position was set manually as a function of free-stream Mach number. Tests were also conducted with the ramp positioned at a large enough throat area so that the inlet would restart by opening the bypass doors.

The terminal shock controller used during these tests was the single-loop proportional-plus-integral control of figure 10(a) (ω_c = 628 rad/sec) using P_{57} feedback. The setpoint for each duct controller depended only on whether the duct was started or unstarted. For started conditions a high setpoint value was used that gave good recovery over the range of ramp positions. When an unstart was detected, the setpoint was dropped momentarily to a value of zero to drive the control bypass doors open rapidly. By opening the bypass doors the inlet throat becomes choked and buzz is suppressed. After dropping to zero the setpoint begins ramping up to a constant level which is consistent with reasonably high total pressure recovery throughout the unstarted portion of the transient.

Three unstart-restart transients are presented and discussed next. The first two transients show either both ducts or only one duct unstarting for the case when the ramp had to be collapsed to effect the restart. The third transient shows the case with the ramp initially positioned (about 9 percent larger throat area) such that it did not have to be collapsed to effect the restart. These transients show how parameters in both ducts are affected by the three different modes of unstart. They also demonstrate that the terminal shock control worked satisfactorily in spite of the instability problem.

The first unstart-restart transient (both ducts unstarted) is shown in figure 19. The figure shows time histories of various inlet variables (for both ducts) through-

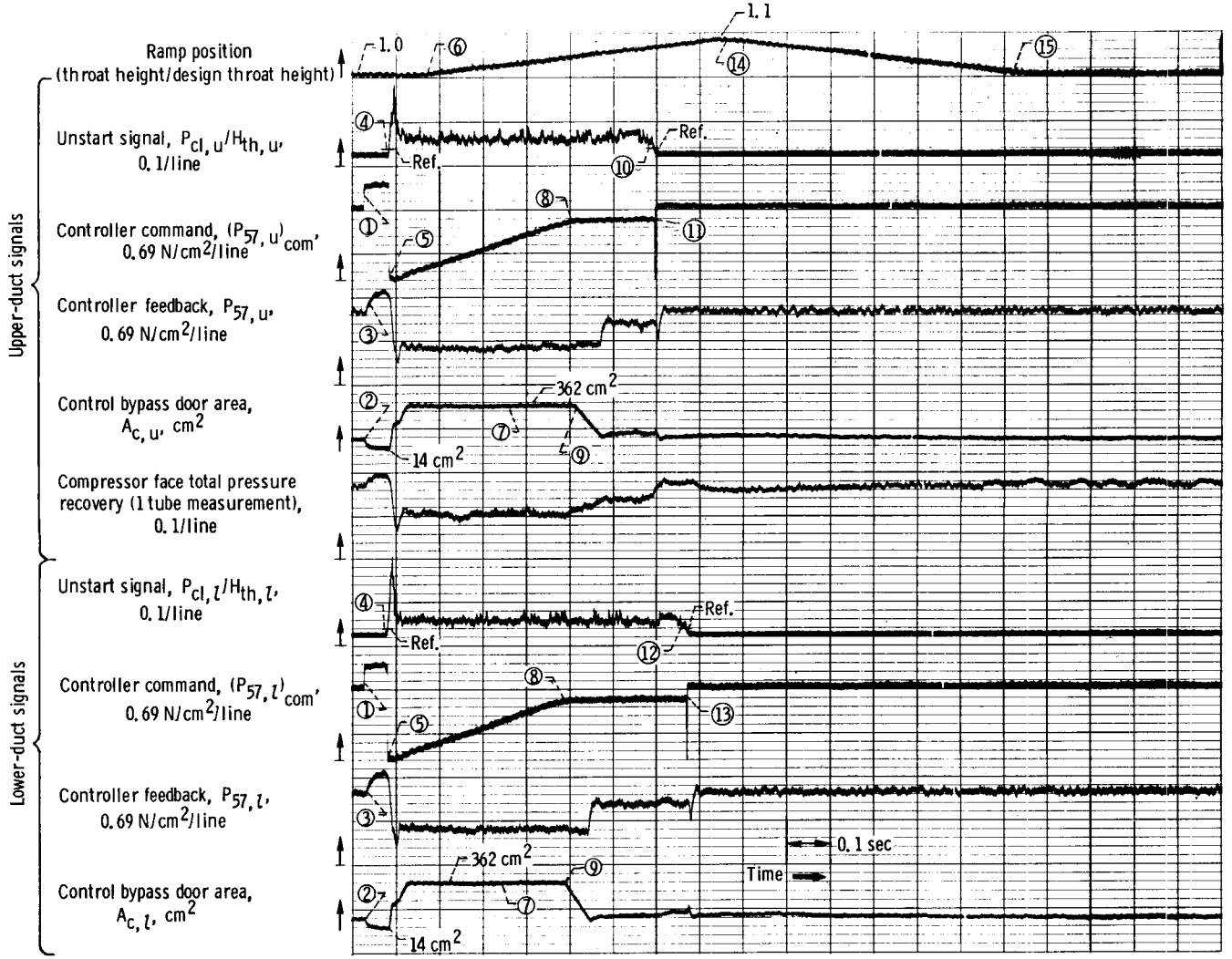

Figure 19. - Controlled unstart-restart transient with both ducts unstarted. Mach 2.7; angle of attack, 0°. (Circled numbers denote main events of transient and correspond to numbered descriptions in text (p. 26).)

out the transient. (The arrows at the left of the figure indicate the direction of increasing magnitude and the baselines - for those arrows that have them - are at zero magnitude.)

The main events of the transient are as follows - the numbers correspond to the circled numbers on the figure:

(1) Inlet unstart is initiated in both ducts by pulsing the controller setpoints, as can be seen in the $(P_{57,u})_{com}$ and $(P_{57,\ell})_{com}$ traces.

(2) Control bypass doors in both ducts start to close in response to the pulse increase in controller setpoint.

(3) Duct pressures start to increase in response to the decrease in bypass door airflow.

(4) Unstart occurs almost simultaneously in both ducts, as indicated by a large drop in duct pressures and a rise in both duct unstart pressure ratios.

(5) Upon sensing of unstart the terminal shock controller setpoint drops to zero (both ducts) and begins ramping back to a higher value.

(6) Also upon unstart the inlet ramp begins to collapse, increasing the ratio of throat- to capture-flow area.

(7) The control doors should have started closing because the terminal shock control command exceeds the feedback. However, some of the analog computer amplifiers in the controller are saturated as a result of the large error after unstart. The problem can be eliminated by using diode limiters on the amplifiers.

(8) The controller setpoints reach the constant level for unstarted conditions.

(9) The controller amplifiers come out of saturation and the control doors start closing in response to the error in P_{57}.

(10) The upper duct restarts first.

(11) The upper-duct controller setpoint switches back to the value for started conditions.

(12) The lower duct restarts approximately 0.075 second after the upper duct.

(13) The lower-duct controller setpoint switches back to the value for started conditions.

(14) The ramp begins returning to the design position.

(15) The inlet has returned to its initial condition.

The time between sensing of unstart and sensing of restart (lower duct) was about 0.7 second, and the total time for the unstart-restart cycle was about 1.4 seconds.

These times were limited by the rate at which the ramp was collapsed and raised. A conservative rate was used to prevent damage to rubber seals between internal compartments of the ramp.

The second unstart-restart transient is shown in figure 20. This case differs from the first in that only the upper duct was unstarted. There are no significant differences in the upper-duct parameters between figures 19 and 20. The lower duct appears to be almost unaffected by the upper-duct unstart transient. Some variation in the lower-duct control bypass door position throughout the restart cycle can be noted. This is a result of the doors maintaining a constant value of P_{57} while the

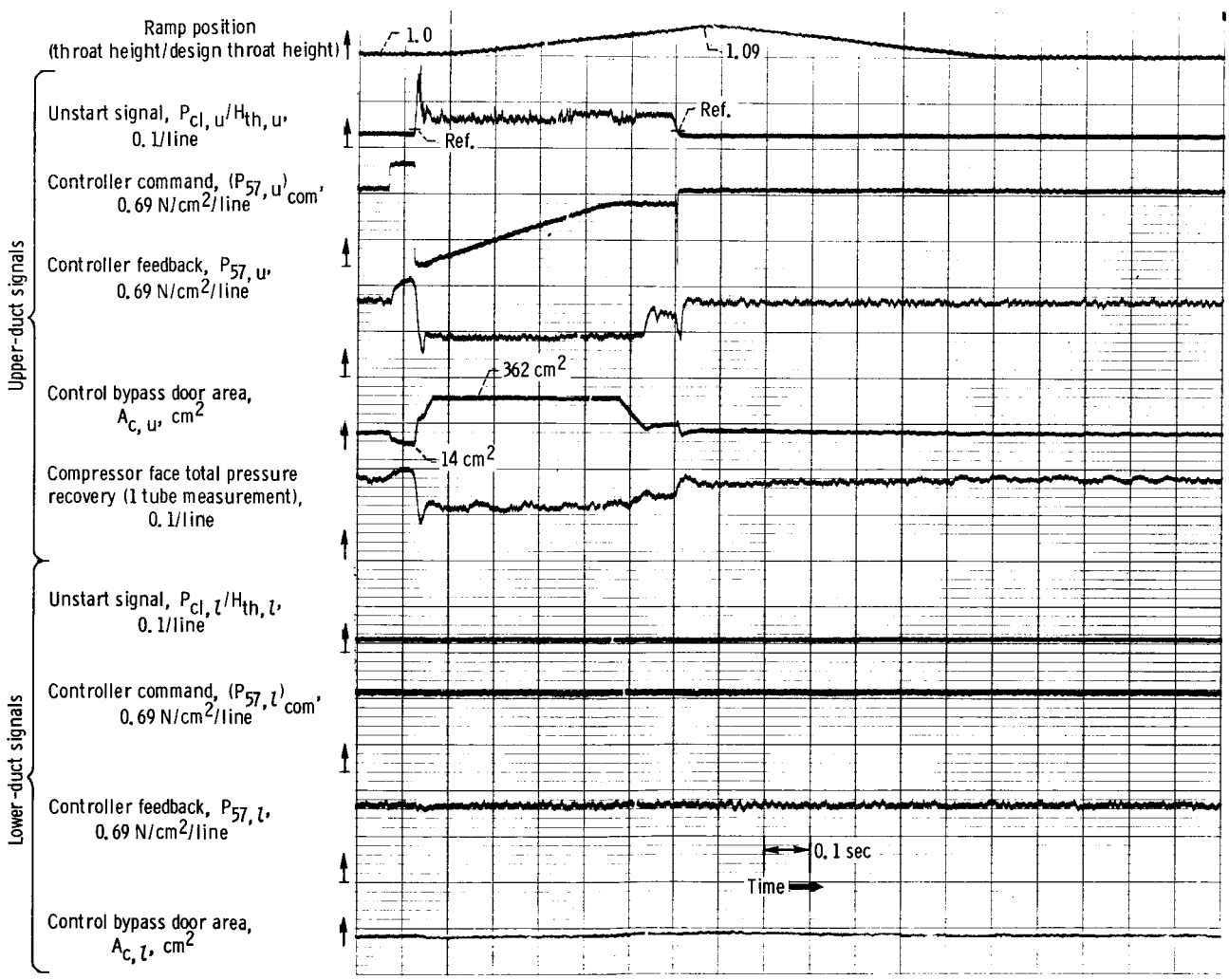

Figure 20. - Controlled unstart-restart transient with unstart in upper duct only. Mach 2.7; angle of attack, 0^0.

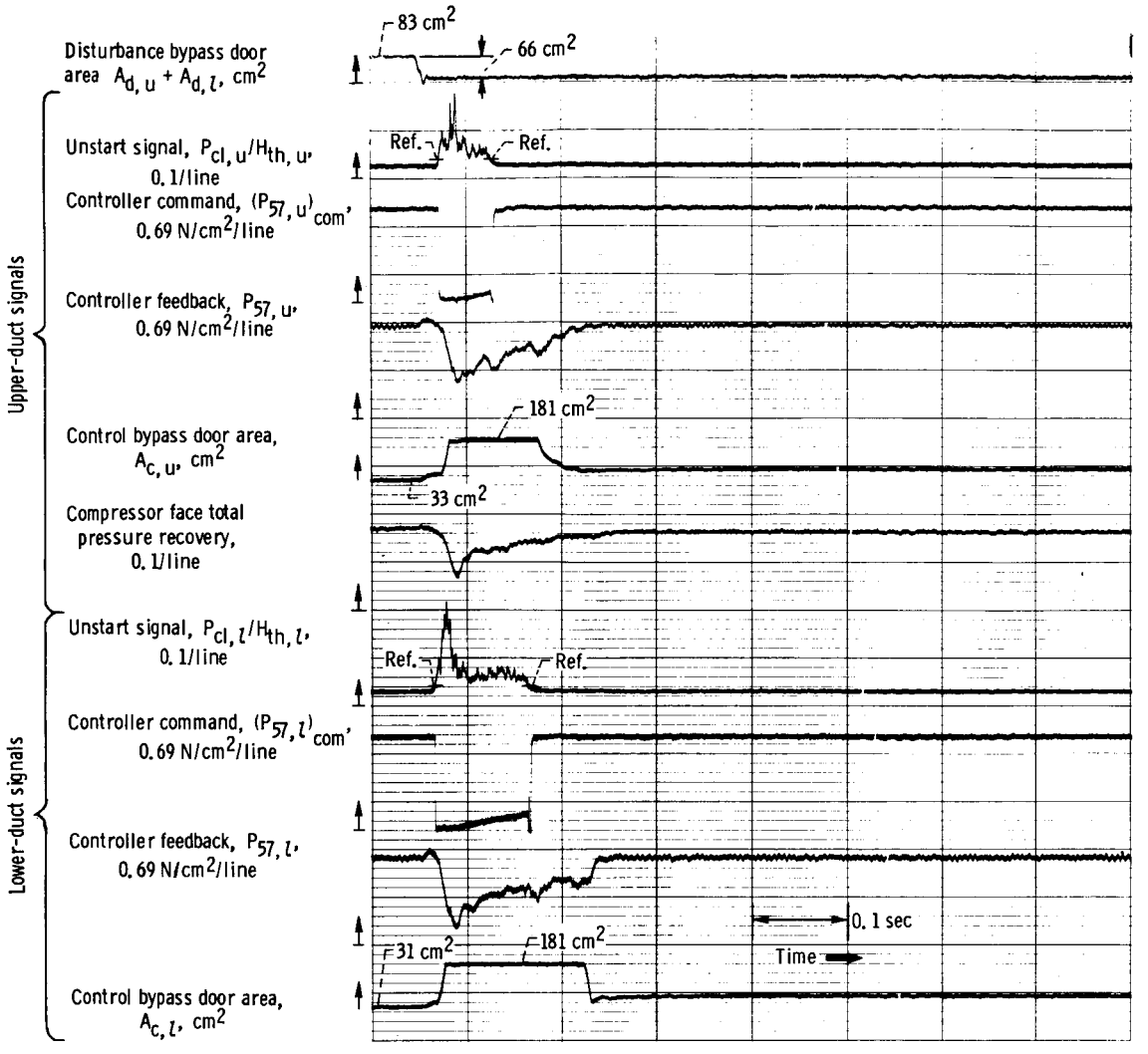

Figure 21. - Controlled unstart-restart transient with ramp at self-starting position (throat height/design throat, 1.09) and both ducts unstarted. Mach 2.7; angle of attack, 0°.

ramp collapses and then returns to the design position. The restart and total cycle times were about the same as for the previous test.

The last unstart-restart transient is shown in figure 21. In this case the ramp was initially set at a self-starting position. That is, if an unstart occurs, the only action required to restart the inlet is to have sufficient bypass door opening. Thus, the need for providing a logic signal to the ramp control is eliminated, simplifying the control system.

For this test, one door in each duct was used for disturbance and the other for

control. The terminal shocks were initially placed on the verge of unstart. Although the shocks were initially farther forward than for the cases of figures 19 and 20, the compressor face total pressure recovery was lower. The reason is that the inlet was operating at a higher throat Mach number (due to the larger throat area) and thus lower pressure recovery in the case of figure 21. The recovery loss was about 4 percent with the ramp at this self-starting position compared to what it was with the ramp at the design position. A step in disturbance bypass door area caused both ducts to unstart. Both ducts unstarted almost simultaneously. Upon unstart, the controller setpoint for both ducts dropped to zero (as scheduled) and began ramping back to a higher value. The bypass doors responded by opening rapidly. The upper duct restarted first (in about 0.06 sec). The lower duct restarted in about 0.1 second. The control doors were somewhat more open at the end of the transient to compensate for the step in disturbance door area. This was an extremely fast transient compared to those shown in figures 19 and 20.

SUMMARY OF RESULTS

In tests of an inlet terminal shock control system and an inlet restart control system, an inherent instability in inlet shock position was discovered. The instability resulted in noisy feedback control signals which restricted the terminal shock control system performance that was achieved. The noisy signals did not seem to limit the restart capability of the control system.

Terminal Shock Control Systems

Airflow coupling between the inlet's two ducts was found to be very small, both dynamically and in steady state. When the two ducts were controlled independently and a disturbance was introduced in only one duct, there appeared to be no interaction between the two control systems. The two ducts were thus assumed to be independently controllable, and subsequent closed-loop responses of the terminal shock control systems were measured only in one duct.

Proportional-plus-integral-type controllers were tested by using either a throat exit static pressure or the output of an electronic shock position sensor as the feedback signal. The pressure feedback provided somewhat better control, as indicated in the following table. A shock position sensor does have the advantage of directly measuring the controlled variable. Thus, it might not require scheduling of the

Feedback signal	1-Hertz closed-loop amplitude, percent of steady-state open-loop amplitude	Attenuation below open-loop values, Hz	Peak closed-loop amplitude, percent of steady-state open-loop amplitude
Pressure	7.4	0 to 15	85.0
Shock sensor	8.4	0 to 8.5	102.0

feedback variable as a function of flight conditions. This consideration may outweight the somewhat poorer shock sensor control dynamic performance.

A proportional loop feeding back a diffuser exit pressure was added to improve control performance by having a signal closer to the disturbance. The resulting closed-loop frequency response data did indicate an improvement. However, the proportional loop propagated more noise through the control system and resulted in unacceptable bypass door activity. Three bypass door failures occurred during the experimental program that were attributed to the noise problem. Thus, a pure proportional control loop was eliminated from the control system.

Restart Control System

The inlet restart control system kept the terminal shock control loop closed throughout the unstart-restart transient. This was accomplished by scheduling the shock controller command signal. Restarts were successful if either one or both inlet ducts were unstarted. When an unstart occurred with the inlet ramp at its design position, it was necessary to collapse the ramp to effect a restart. Total time from unstart back to initial conditions was about 1.4 seconds, because of the conservative collapsing rate used to protect rubber seals between interior compartments of the ramp. If an unstart occurred in only one duct, there was no major effect upon the opposite duct.

A restart test was also conducted with the ramp positioned to provide a throat area 9 percent larger than design so that the inlet would restart by opening the overboard bypass doors. The total unstart-restart cycle occurred in approximately 0.1 second. Thus, operating with the ramp at the so-called self-starting position results in a somewhat simpler control system and has the advantage of recovering to

design conditions much more quickly than when the ramp must be collapsed. However, the advantage may be offset by the increased throat size (and hence throat Mach number), which resulted in a compressor face total pressure recovery loss of aboug 4 percent relative to the design operating condition.

Lewis Research Center,
National Aeronautics and Space Administration,
Cleveland, Ohio, April 13, 1973,
501-24.

APPENDIX - SYMBOLS

A	bypass door area, cm^2
AR	amplitude ratio, dimensionless
a,b,. . ., h	static pressure taps on inlet cowl surface (also pressures measured at taps)
E	input signal to bypass door servomechanisms, V
ESP	output of electronic shock position sensor, V
G	frequency-dependent portion of transfer function
H	total pressure, N/cm^2
K	steady-state gain term
P	static pressure, N/cm^2
Q	noise-penalty weighting factor
s	Laplace variable, 1/sec
T	total temperature, K
W	corrected airflow, $w\sqrt{\theta}/\delta$, kg/sec
w	actual airflow, kg/sec
X	position, cm
Δ	incremental change in variable
δ	$H/(10.1\ N/cm^2)$
θ	$T/(288.2\ K)$
ω	frequency, rad/sec
Subscripts:	
a,b,. . ., h	pressures measured at pressure taps
b	overboard bypass
c	controller
cl	cowl lip static pressure measurement (fig. 4)
com	commanded value
cs	control using shock sensor output for feedback
c57	control using throat exit static pressure P_{57} feedback
c87	control using diffuser exit static pressure P_{87} feedback
d	disturbance
ℓ	inlet lower duct
s	terminal shock
ss	steady state

td	transducer
th	throat total pressure measurement (fig. 4)
u	inlet upper duct
57	inlet station 57 cm downstream of cowl lip
87	inlet station 87 cm downstream of cowl lip

REFERENCES

1. Sanders, Bobby W.; and Mitchell, Glenn A.: Increasing the Stable Operating Range of a Mach 2.5 Inlet. Paper 70-686, AIAA, June 1970.
2. Chun, K. S.; and Burr, R. H.: A Control System Concept for an Axisymmetric Supersonic Inlet. J. Aircraft, vol. 6, no. 4, July-Aug. 1969, pp. 306-311.
3. Neiner, George H.; Crosby, Michael J.; and Cole, Gary L.: Experimental and Analytical Investigation of Fast Normal Shock Position Controls for a Mach 2.5 Mixed-Compression Inlet. NASA TN D-6382, 1971.
4. Neiner, George H.; Cole, Gary L.; and Arpasi, Dale J.: Digital-Computer Normal-Shock-Position and Restart Control of a Mach 2.5 Axisymmetric Mixed-Compression Inlet. NASA TN D-6880, 1972.
5. Cole, Gary L.; Neiner, George H.; and Crosby, Michael J.: An Automatic Restart Control System for an Axisymmetric Mixed-Compression Inlet. NASA TN D-5590, 1969.
6. Baumbick, Robert J.; Neiner, George H.; and Cole, Gary L.: Experimental Dynamic Response of a Two-Dimensional, Mach 2.7, Mixed-Compression Inlet. NASA TN D-6957, 1972.
7. Dustin, Miles O.; and Cole, Gary L.: Performance Comparison of Three Normal-Shock Position Sensors for Mixed-Compression Inlets. NASA TM X-2739, 1973.
8. Wasserbauer, Joseph F.: Dynamic Response of a Mach 2.5 Axisymmetric Inlet with Engine or Cold Pipe and Utilizing 60 Percent Supersonic Internal Area Contraction. NASA TN D-5338, 1969.
9. Neiner, George H.: Servosystem Design of a High-Response Slotted-Plate Overboard Bypass Valve for a Supersonic Inlet. NASA TN D-6081, 1970.
10. Batterton, Peter G.; and Zeller, John R.: Performance Characteristics of Improved Servoamplifier for Electrohydraulic Control Systems. NASA TM X-2167, 1971.
11. Zeller, John R.: Analysis of Dynamic Performance Limitations of Fast Response (150 to 200 Hz) Electrohydraulic Servos. NASA TN D-5388, 1969.
12. Webb, John A., Jr.; Mehmed, Oral; and Hiller, Kirby W.: Improved Design of a High-Response Slotted-Plate Overboard Bypass Valve for Supersonic Inlets. NASA TM X-2812, 1973.

13. Zeller, John R.; Lehtinen, Bruce; Geyser, Lucille C.; and Batterton, Peter G.: Analytical and Experimental Performance of Optimal Controller Designs for a Supersonic Inlet. NASA TN D-7188, 1973.